

## Electronic supplementary information

### **Optimization of the synthesis of quinoline-based neutral cyclometalated iridium complexes *via* microwave irradiation: Design of light-harvesting and emitting complexes using bulky quinolines**

Carlos A. Echeverry-Gonzalez,<sup>a</sup> Carlos E. Puerto-Galvis,<sup>a</sup> Carlos H. Borca,<sup>b</sup> Martín A. Mosquera,<sup>c</sup> Andrés F. Luis-Robles,<sup>a</sup> and Vladimir V. Kouznetsov \*<sup>a</sup>

<sup>a</sup> Laboratorio de Química Orgánica y Biomolecular, CMN, Universidad Industrial de Santander, Parque Tecnológico Guatiguará, Km 2 vía refugio, Piedecuesta, A.A. 681011, Colombia.

<sup>b</sup> School of Chemistry and Biochemistry, Georgia Institute of Technology, 901 Atlantic Drive NW, Atlanta, Georgia, 30332, United States

<sup>c</sup> Department of Chemistry, Northwestern University, 2145 Sheridan Road, Evanston, Illinois 60208, United States

## Content

1.	Optimization of MW methodology .....	3
2.	Experimental section.....	3
2.1.	Quinoline ligands.....	4
2.2.	General synthetic procedure for neutral cyclometalated iridium complexes .....	5
2.3.	<sup>1</sup> H and <sup>13</sup> C NMR of the synthesized complexes .....	6
2.3.1.	Complex <b>4a</b> .....	6
2.3.2.	Complex <b>4ab</b> .....	7
2.3.3.	Complex <b>4b</b> .....	8
2.3.4.	Complex <b>4c</b> .....	9
2.3.5.	Complex <b>4d</b> .....	10
2.3.6.	Complex <b>4e</b> .....	11
2.3.7.	Complex <b>4f</b> .....	12
2.3.8.	Complex <b>4g</b> .....	13
2.3.9.	Complex <b>4h</b> .....	14
2.3.10.	Complex <b>4i</b> .....	15
2.4.	Theoretical and Photophysical characterization of complexes <b>4g-i</b> .....	16
2.4.1.	Solvatochromic study .....	16
2.4.2.	Optimized structures.....	17
2.4.3.	Transition excited states.....	18
3.	Relative quantum yields.....	19
4.	References.....	20

## 1. Optimization of MW methodology

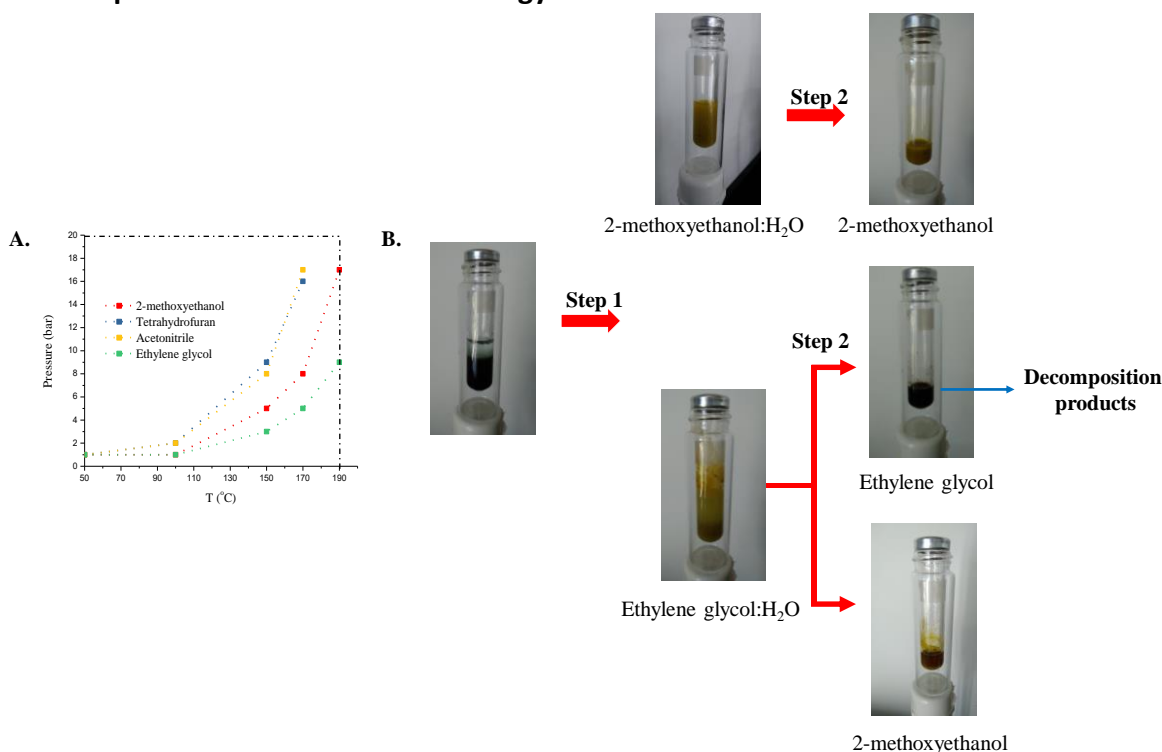


**Fig S1.** Optimization of methodology for the synthesis of neutral cyclometalated iridium complexes: **A.** Pressure vs Temperature graph as a result of irradiating with MW the mixtures of the respective solvents with water (3:1); **B.** Photographic record of each step in the synthesis of complex **4** using 2-methoxyethanol and ethylene glycol.

## 2. Experimental section

**General.** The synthesis of neutral cyclometalated iridium complexes was performed using a Biotage® initiator Microwave Synthesizer. All reagents and solvents were used as purchased. All air-sensitive reactions were carried out under argon atmosphere. Flash chromatography was performed using silica gel (Merck, Kieselgel 60, 230-240 mesh or Scharlau 60, 230-240 mesh). Analytical thin layer chromatography (TLC) was performed using aluminum coated Merck Kieselgel60 F254 plates. NMR spectra were recorded on a Bruker Avance 400 (<sup>1</sup>H: 400 MHz; <sup>13</sup>C: 100 MHz) spectrometer at 298 K using partially deuterated solvents as internal standards. Coupling constants (J) are denoted in Hz and chemical shifts ( $\delta$ ) in ppm. Multiplicities are denoted as follows: s = singlet, d = doublet, t = triplet, m = multiplet, br = broad. UV-Vis spectra were recorded on a Genesys 10s spectrophotometer using toluene, dichloromethane, acetonitrile and dimethylformamide as solvents. Emission spectra were recorded on a Photon Technology International spectrophotometer using dichloromethane and acetonitrile as solvents. Matrix Assisted Laser Desorption Ionization (coupled to a Time-Of-Flight analyzer) experiments (MALDI-TOF) were recorded on a HP1100MSD spectrometer and a Bruker REFLEX spectrometer respectively.

## 2.1. Quinoline ligands

C<sup>N</sup> ligands based on quinoline derivatives were synthesized according to literature reports. Spectroscopic data for chemistry validation were performed by NMR as can be seen in Table S1.

**Table S1.** C<sup>N</sup> ligands obtained through conventional protocols

Ligand	Structure	Characterization	Reference
<b>1b</b>		White solid (138.0 mg, 31%). <sup>1</sup> H NMR (400 MHz, CDCl <sub>3</sub> ) δ: 8.22 – 8.15 (m, 4H), 7.92 (dd, J = 8.6, 0.9 Hz, 1H), 7.59 – 7.44 (m, 5H) ppm.	<sup>1</sup>
<b>1c</b>		White solid (180.6 mg, 44%). <sup>1</sup> H NMR (400 MHz, CDCl <sub>3</sub> ) δ: 8.27 – 8.17 (m, 4H), 7.91 (d, J = 8.6 Hz, 1H), 7.86 (dd, J = 8.1, 1.5 Hz, 1H), 7.76 (m, 1H), 7.59 – 7.47 (m, 4H) ppm.	<sup>1</sup>
<b>1d</b>		White solid (282.0 mg, 50%). <sup>1</sup> H NMR (400 MHz, CDCl <sub>3</sub> ) δ: 8.28 (d, J = 8.5 Hz, 1H), 8.25 – 8.20 (m, 2H), 7.94 (d, J = 8.4 Hz, 1H), 7.86 (s, 1H), 7.79 – 7.75 (m, 1H), 7.62 – 7.47 (m, 9H) ppm	<sup>2</sup>
<b>1e</b>		Yellow solid (300.0 mg, 60%). <sup>1</sup> H NMR (400 MHz, CDCl <sub>3</sub> ) δ: 8.50 (dd, J = 7.8, 1.6 Hz, 1H), 8.10 (d, J = 8.9 Hz, 1H), 7.61 (dd, J = 8.9, 2.3 Hz, 1H), 7.56 (t, J = 6.8 Hz, 3H), 7.44 (d, J=2.3 Hz, 1H), 7.40-7.35 (m, 1H), 7.29 (dd, J = 7.6, 1.7 Hz, 2H), 7.18 (t, J = 7.5 Hz, 1H), 6.98 (d, J = 7.7 Hz, 1H), 5.09 (s, 2H) ppm. <sup>13</sup> C NMR (100 MHz, CDCl <sub>3</sub> ) δ: 157.4, 149.2, 146.6, 143.1, 134.3, 132.2, 132.1, 131.3, 130.3, 129.3 (2), 129.1 (2), 129.0, 127.9, 125.8, 125.1, 123.8, 123.3, 122.7, 117.3, 66.7 ppm	---
<b>1f</b>		Yellow solid (250.0 mg, 72%). <sup>1</sup> H NMR (400 MHz, CDCl <sub>3</sub> ) δ: 8.23–8.18 (m, 2H), 7.91 (dd, J = 7.4, 6.1 Hz, 2H), 7.74 (d, J = 7.4 Hz, 2H), 6.62–6.46 (m, 10H), 2.50 (s, 3H) ppm.	<sup>3</sup>
<b>1g</b>		Yellow solid (482.5 mg, 94%). <sup>1</sup> H NMR (400 MHz, CDCl <sub>3</sub> ) δ: 8.15 – 8.10 (m, 2H), 8.02 (d, J = 9.1 Hz, 1H), 7.94 (dd, J = 8.7, 0.8 Hz, 1H), 7.78 (d, J = 8.6 Hz, 1H), 7.55 – 7.49 (m, 3H), 7.47 – 7.41 (m, 1H), 7.36 – 7.28 (m, 5H), 7.20 – 7.15 (m, 4H), 7.12 – 7.07 (m, 2H) ppm. <sup>13</sup> C NMR (100 MHz, CDCl <sub>3</sub> ) δ: 155.6, 147.5, 145.9, 135.5, 130.5, 129.5, 129.0, 128.8, 128.2, 127.4, 127.3, 124.8, 123.5, 119.3, 118.1 ppm.	---
<b>1h</b>		Beige solid (173 mg, 50%) Uv-vis λ <sub>max</sub> (ε/M <sup>-1</sup> cm <sup>-1</sup> , DCM): 331 (12000), 264 (50000) nm. <sup>1</sup> H NMR (400 MHz, CDCl <sub>3</sub> ) δ: 8.69 – 8.66 (m, 1H), 8.44 (dd, J = 8.5, 1.8 Hz, 1H), 8.24 (d, J = 8.5 Hz, 1H), 8.05 – 7.90 (m, 4H), 7.72 – 7.71 (m, 1H), 7.66 – 7.53 (m, 8H), 2.53 (s, 3H) ppm.	<sup>4</sup>
<b>1i</b>		Beige solid (154 mg, 44%). Uv-vis λ <sub>max</sub> (ε/M <sup>-1</sup> cm <sup>-1</sup> , DCM): 333 (9900), 263 (43000) nm. <sup>1</sup> H NMR (400 MHz, CDCl <sub>3</sub> ) δ: 8.68 – 8.63 (m, 1H), 8.42 (dd, J = 8.6, 1.8 Hz, 1H), 8.32 (ddd, J = 9.0, 5.6, Hz, 1H), 8.06 – 7.97 (m, 3H), 7.97 – 7.89 (m, 1H), 7.67 – 7.50 (m, 9H) ppm.	<sup>4</sup>

## **2.2. General synthetic procedure for neutral cyclometalated iridium complexes**

The synthesis of neutral cyclometalated iridium complexes was performed in two steps via MW irradiation. Step 1:  $\text{IrCl}_3 \cdot x\text{H}_2\text{O}$  (50 mg, 0.17 mmol), C<sup>N</sup> ligand (57.2 mg, 0.37 mmol), Solvent:  $\text{H}_2\text{O}$  (1.4 mL) were irradiated by MW for 30 minutes (Temperature: 190 °C; range of pressure: 18 – 20 bar; High power). Then, the colored product (dimer) was centrifuged (15 min at 4000 rpm) and risen three times with diethyl ether to remove unreacted quinoline derivative. Step 2: Dimer (1 eq.), acetylacetone (6 eq.), sodium carbonate (15 eq.) and solvent (6 mL(eq.) were irradiated by MW for 30 minutes (Temperature: 130 °C; range of pressure: 4 – 5 bar; High power). Then, 2-Methoxyethanol was evaporated to reduced pressure and the reaction crude was purified by  $\text{SiO}_2$  chromatography using dichloromethane as mobile phase.

## 2.3. $^1\text{H}$ and $^{13}\text{C}$ NMR of the synthesized complexes

### 2.3.1. Complex 4a

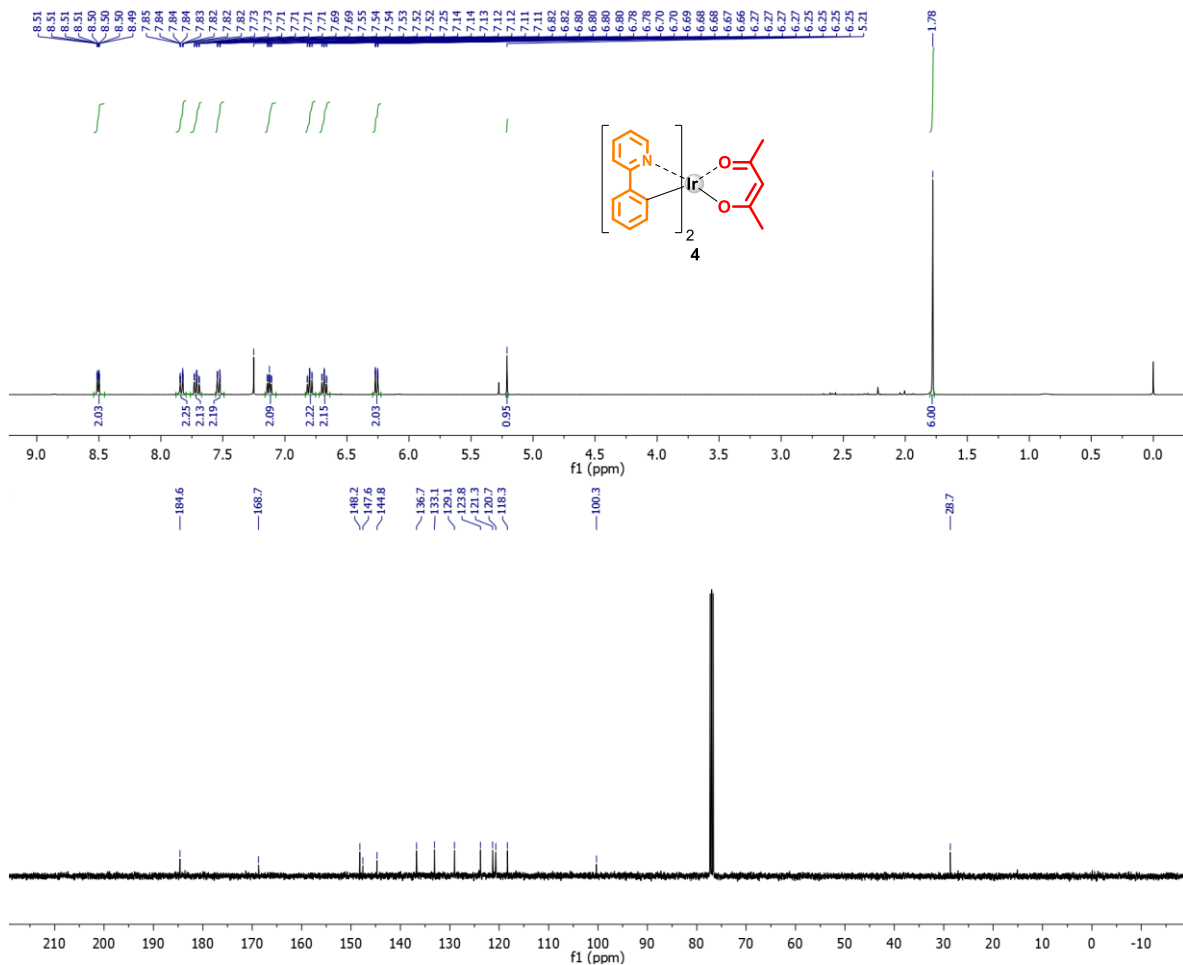


**Fig S2.**  $^1\text{H}$  and  $^{13}\text{C}$  NMR spectra ( $\text{CDCl}_3$ ) of complex 4a.

### 2.3.2. Complex 4ab

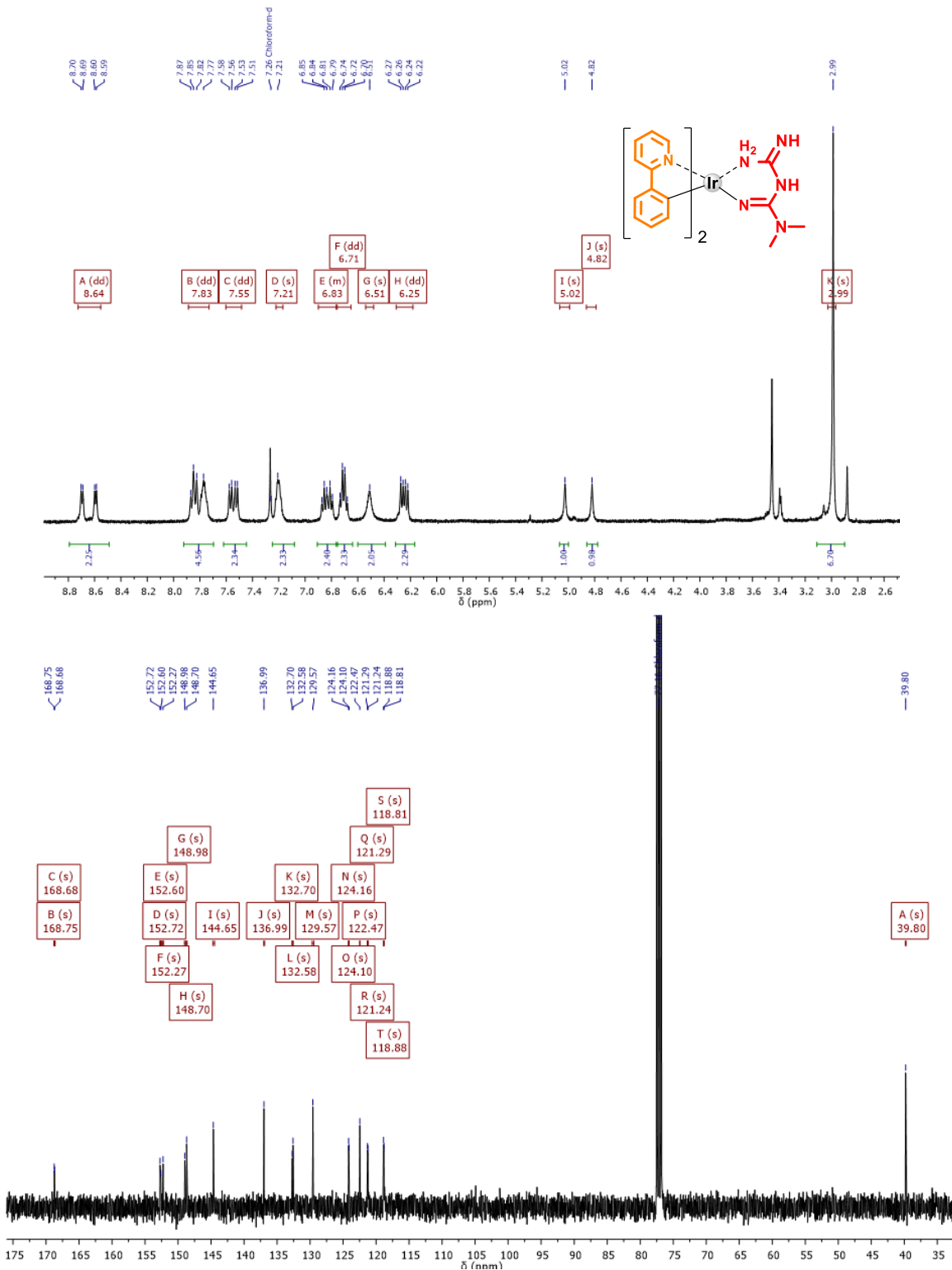


**Fig S3.**  $^1\text{H}$  and  $^{13}\text{C}$  NMR spectra (CDCl<sub>3</sub>) of complex 4ab.

### 2.3.3. Complex 4b

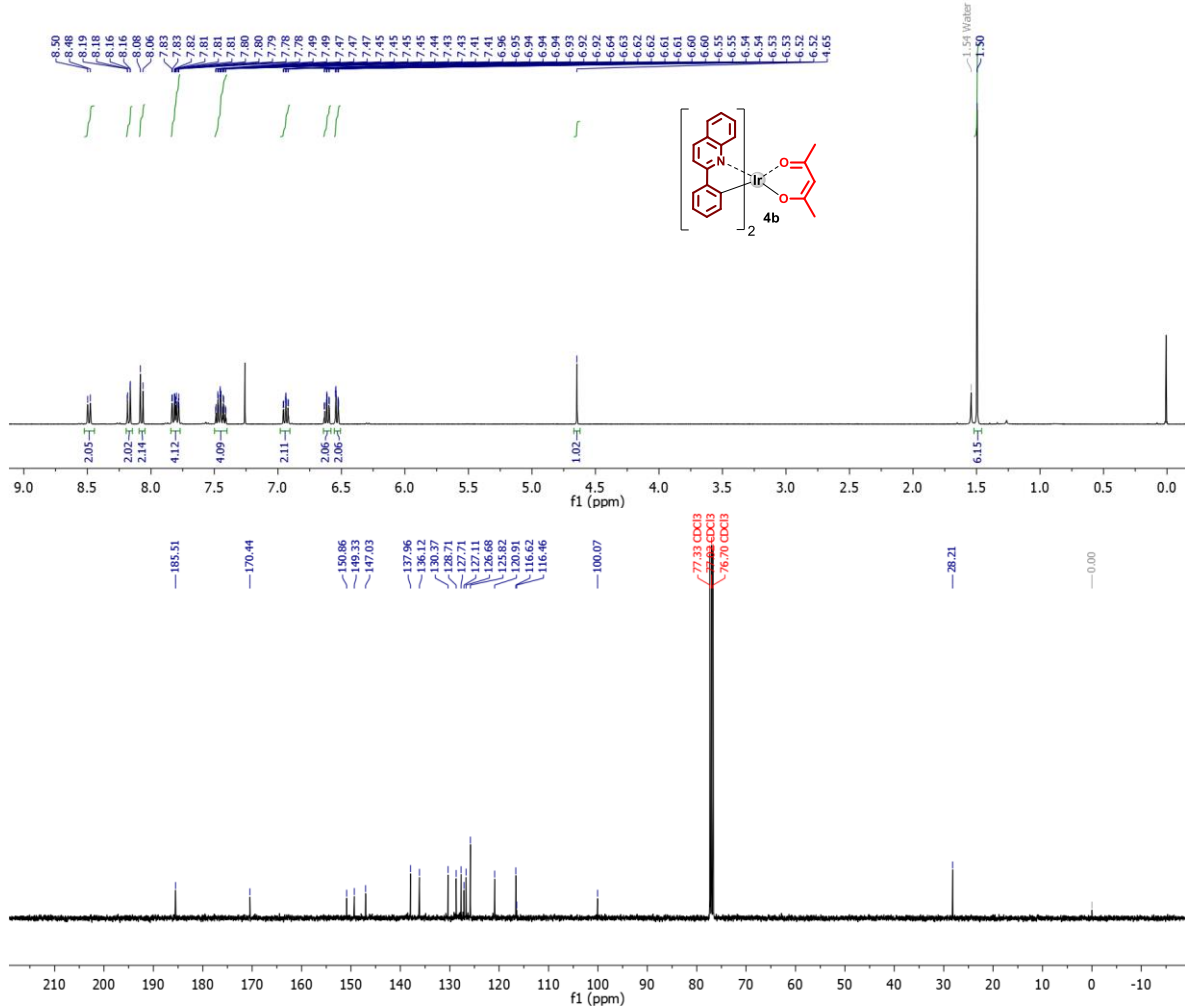


**Fig S4.**  $^1\text{H}$  and  $^{13}\text{C}$  NMR spectra ( $\text{CDCl}_3$ ) of complex **4b**.

### 2.3.4. Complex 4c

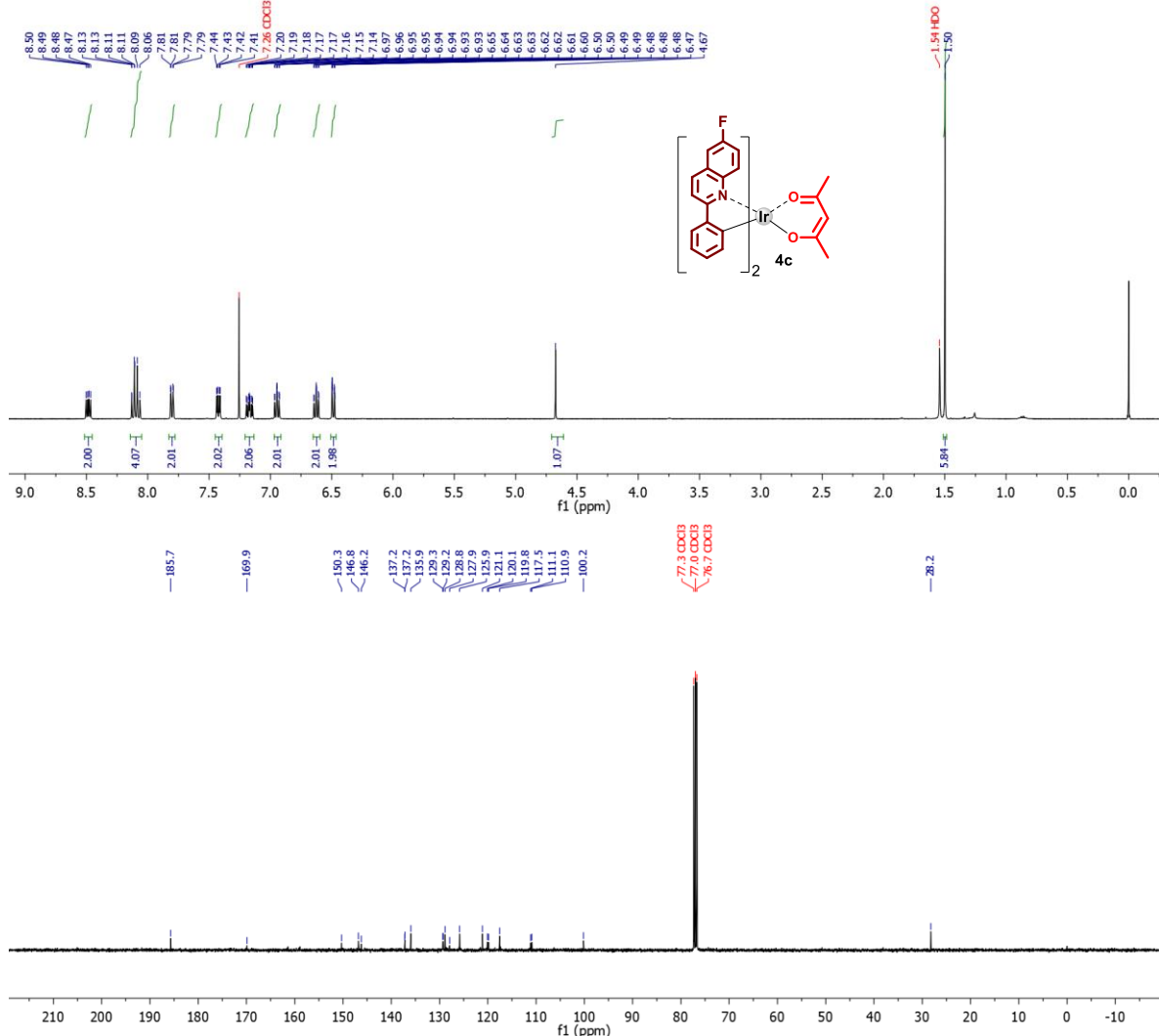


**Fig S5.**  $^1\text{H}$  and  $^{13}\text{C}$  NMR spectra ( $\text{CDCl}_3$ ) of complex 4c.

### 2.3.5. Complex 4d

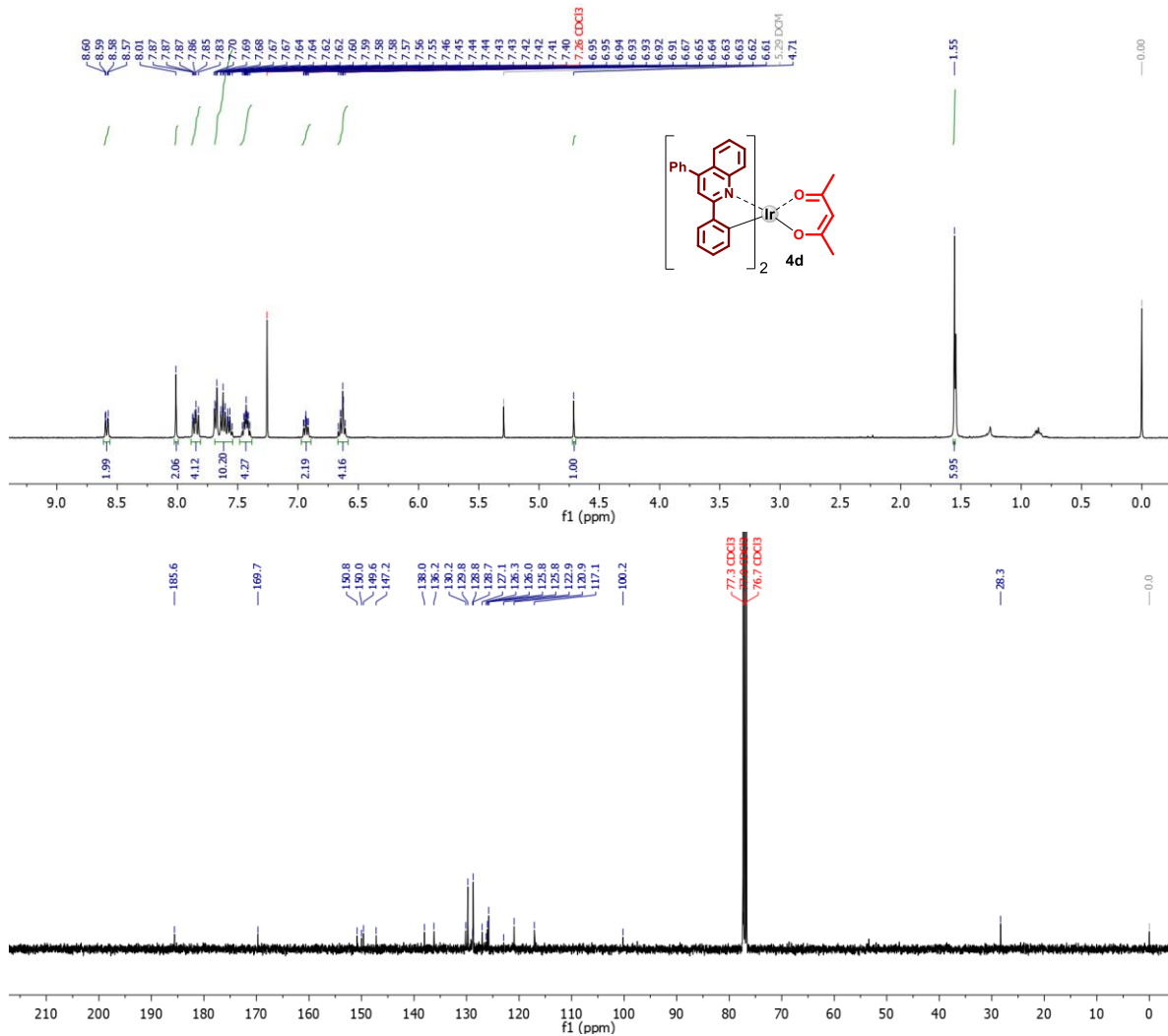


**Fig S6.**  $^1\text{H}$  and  $^{13}\text{C}$  NMR spectra ( $\text{CDCl}_3$ ) of complex **4d**.

### 2.3.6. Complex 4e

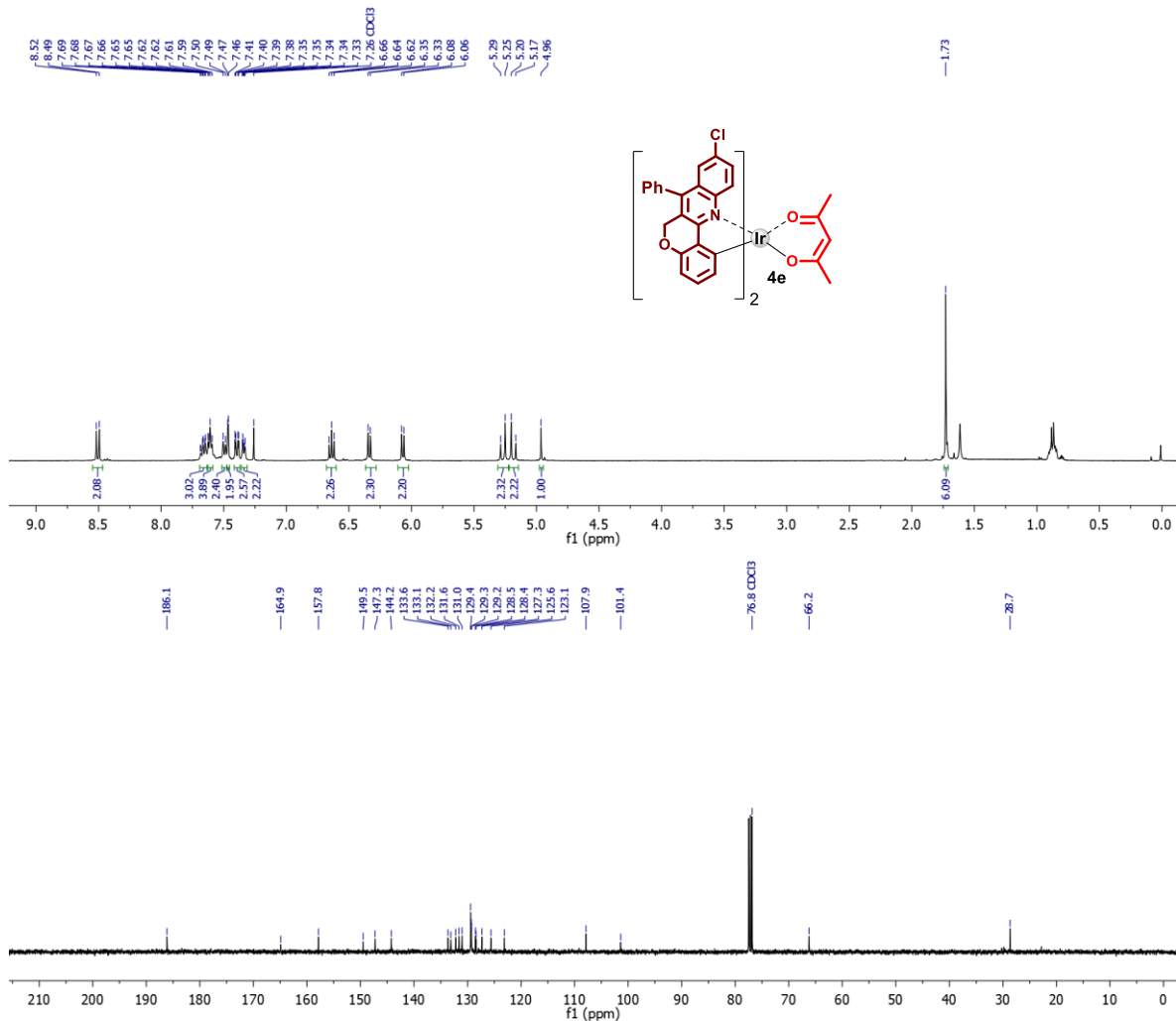


**Fig S7.**  $^1\text{H}$  and  $^{13}\text{C}$  NMR spectra ( $\text{CDCl}_3$ ) of complex **4e**.

### 2.3.7. Complex 4f

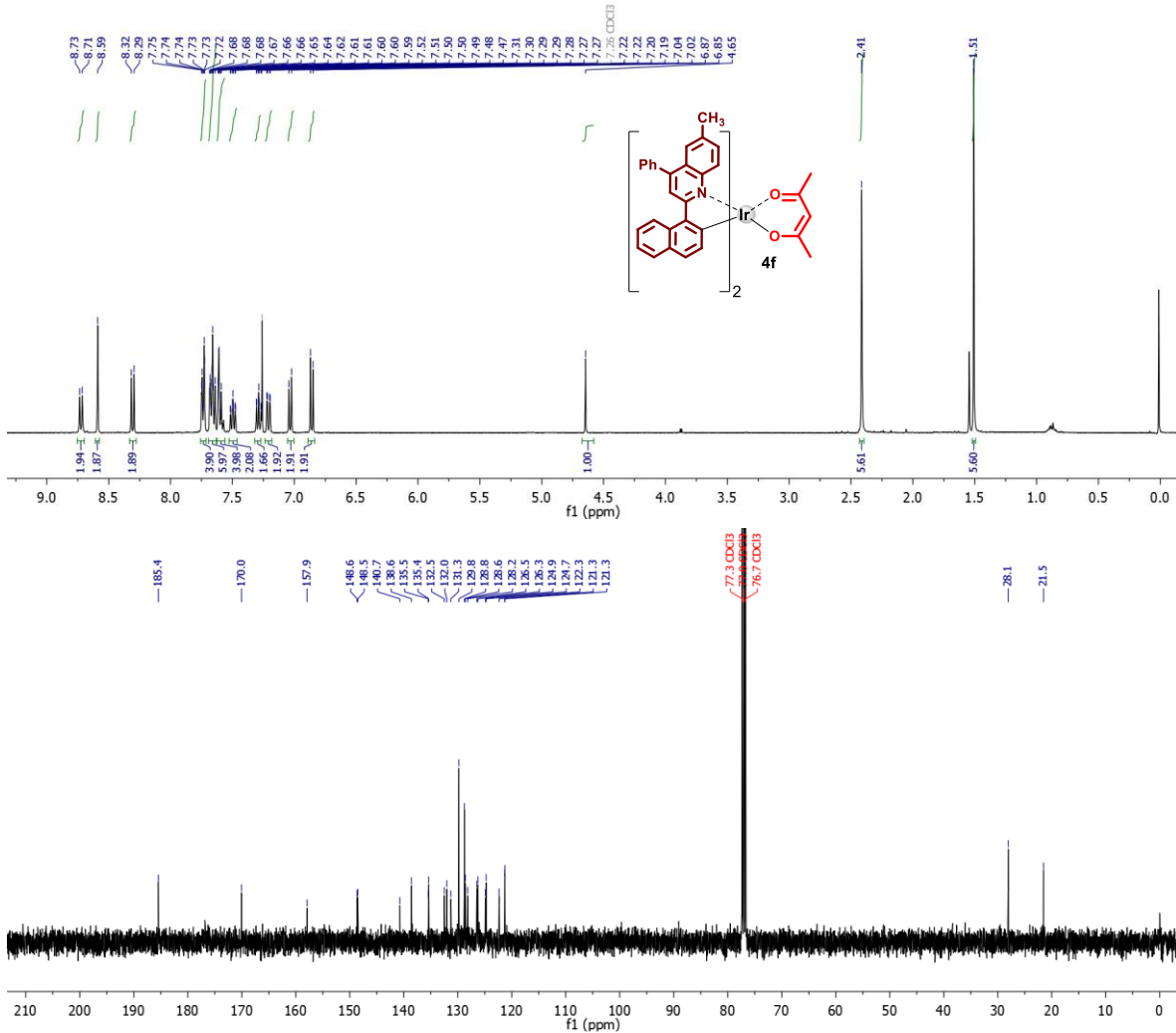


**Fig S8.**  $^1\text{H}$  and  $^{13}\text{C}$  NMR spectra ( $\text{CDCl}_3$ ) of complex **4f**.

### 2.3.8. Complex 4g

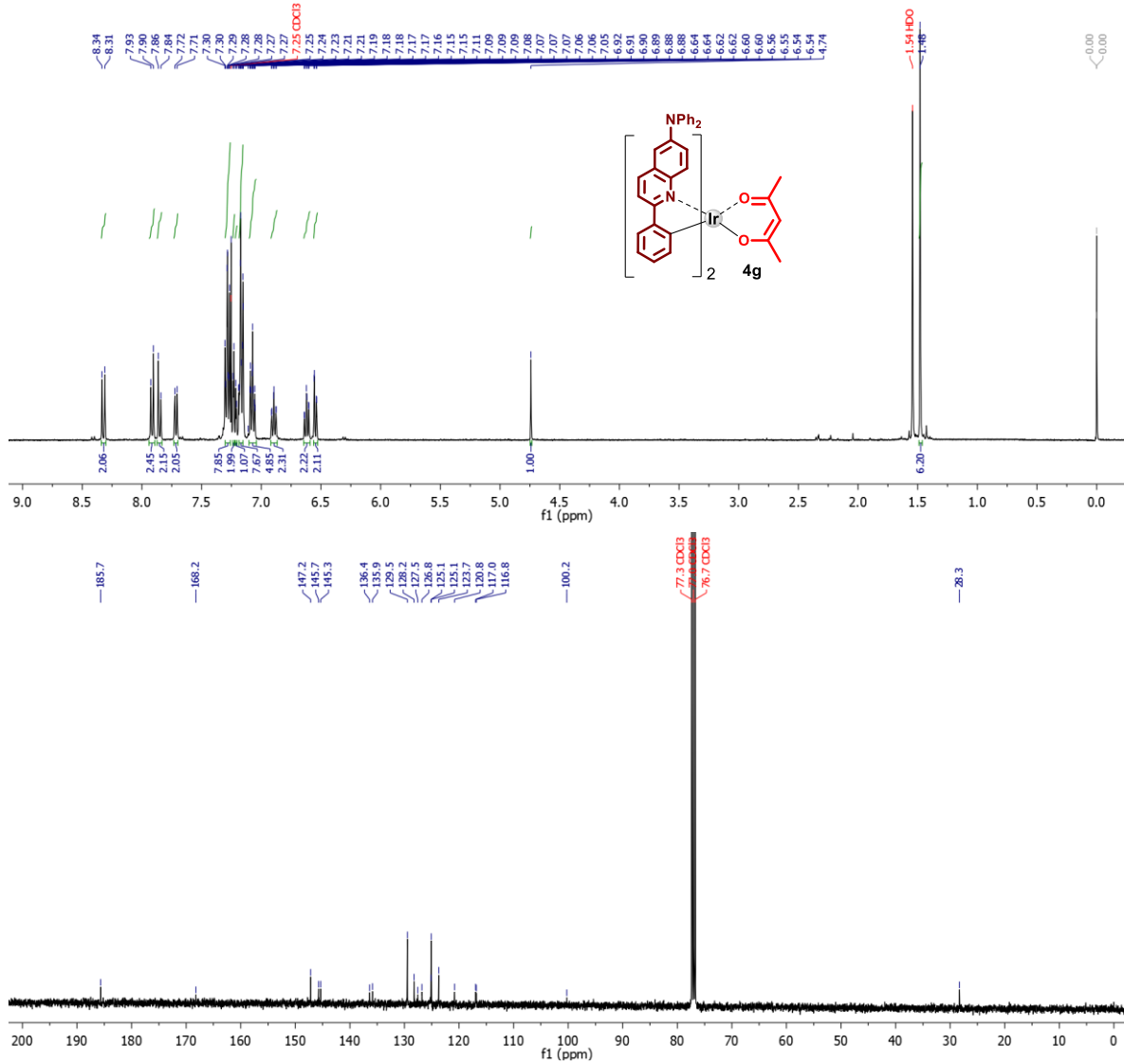


**Fig S9.** <sup>1</sup>H and <sup>13</sup>C NMR spectra (CDCl<sub>3</sub>) of complex 4g.

### 2.3.9. Complex 4h

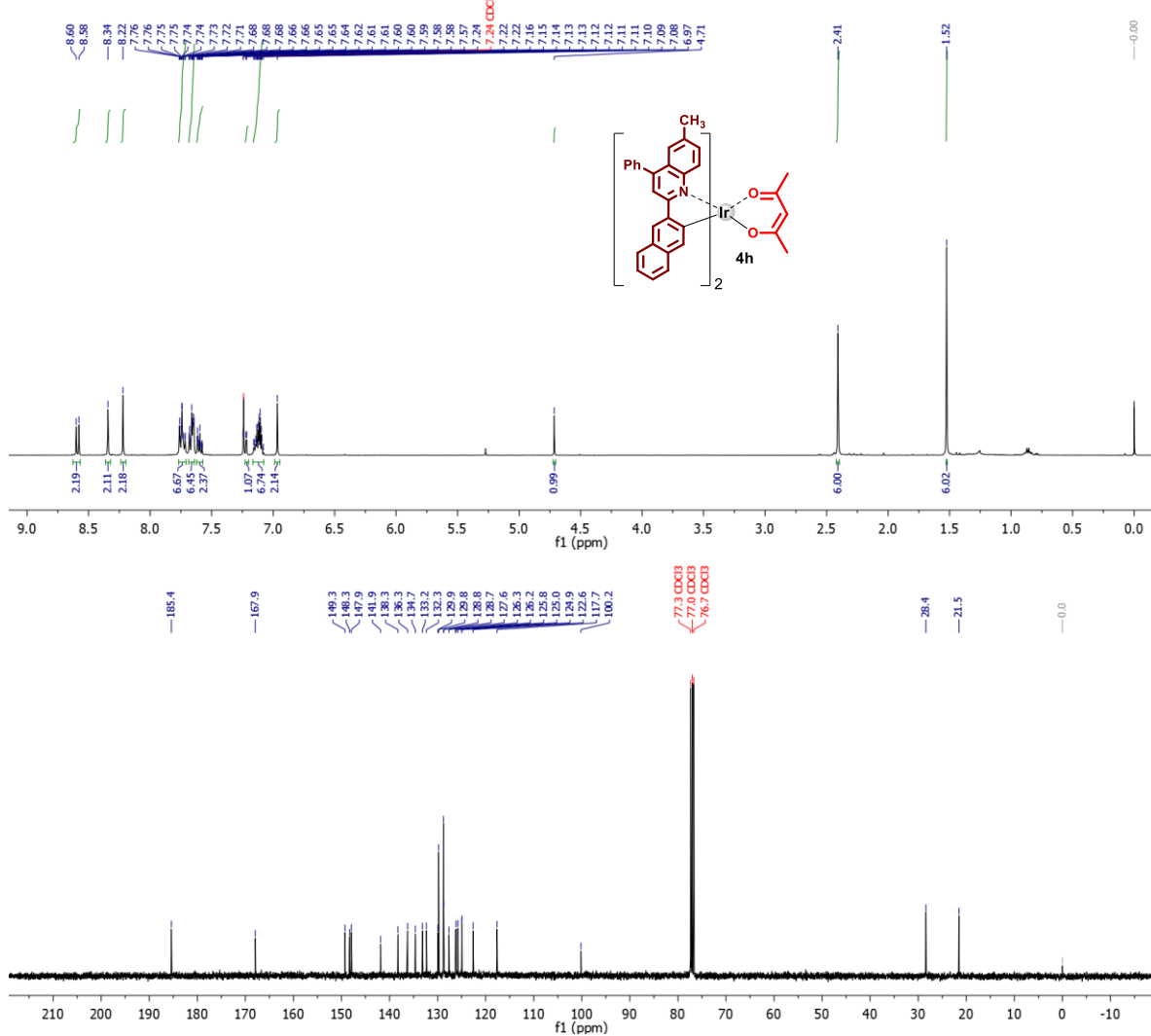


**Fig S10.** <sup>1</sup>H and <sup>13</sup>C NMR spectra ( $\text{CDCl}_3$ ) of complex 4h.

### 2.3.10. Complex 4i

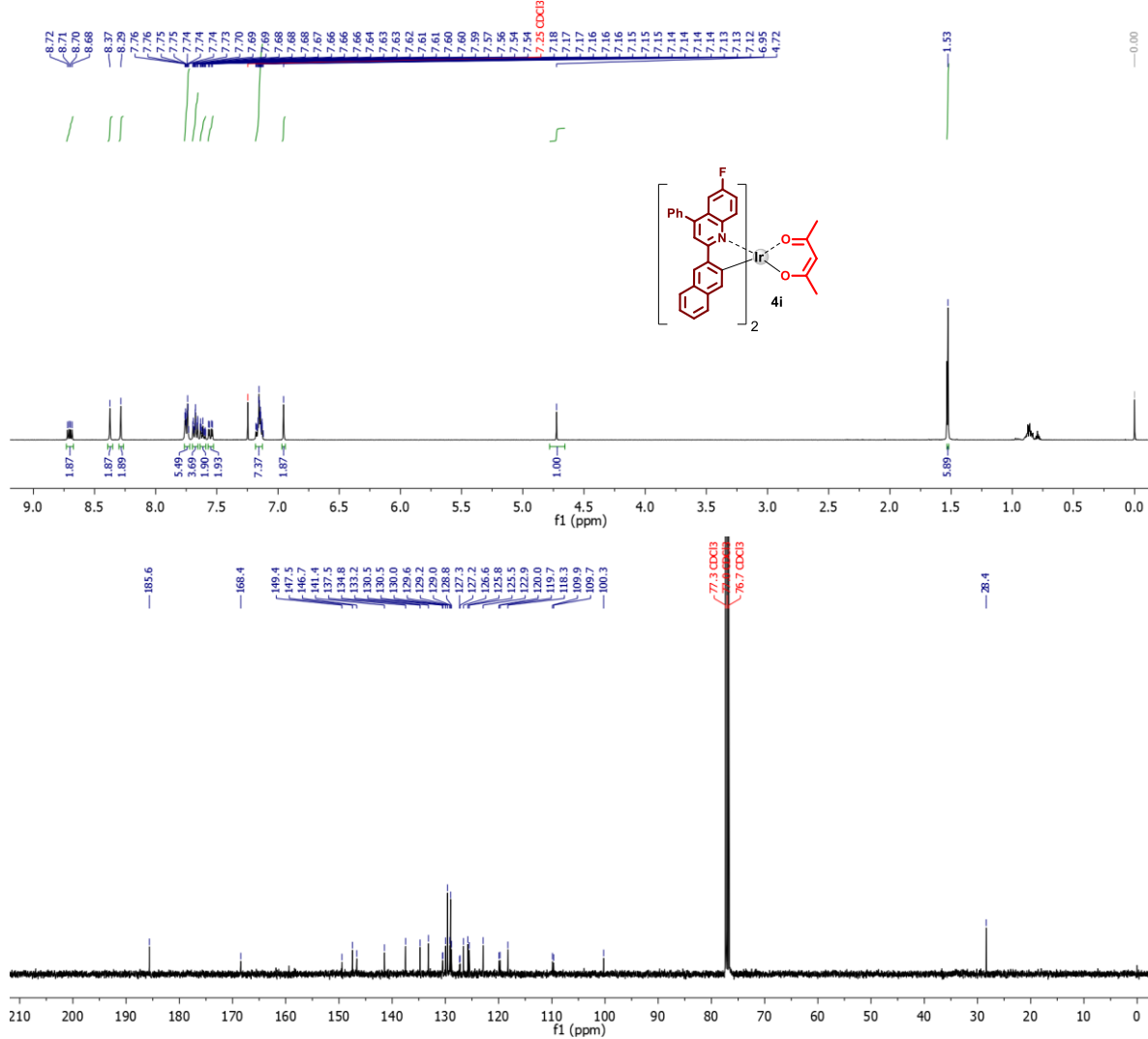


**Fig S11.**  $^1\text{H}$  and  $^{13}\text{C}$  NMR spectra ( $\text{CDCl}_3$ ) of complex **4i**.

## 2.4. Theoretical and Photophysical characterization of complexes 4g-i

### 2.4.1. Solvatochromic study

The absorption spectra for complexes **4g-i** at a concentration of  $1 \times 10^{-5}$  M in toluene, chloroform, dichloromethane, dimethylformamide, acetonitrile and methanol are showed in Fig S12 and data are summarized in Table S2.

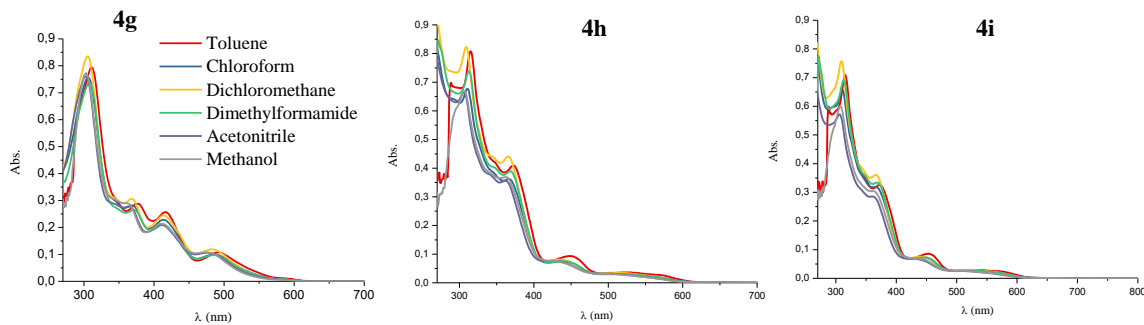


**Fig S12.** Absorption spectra for complexes **4g-i**.

**Table S2.** Photophysical characteristics of the new iridium complexes in different solvents.

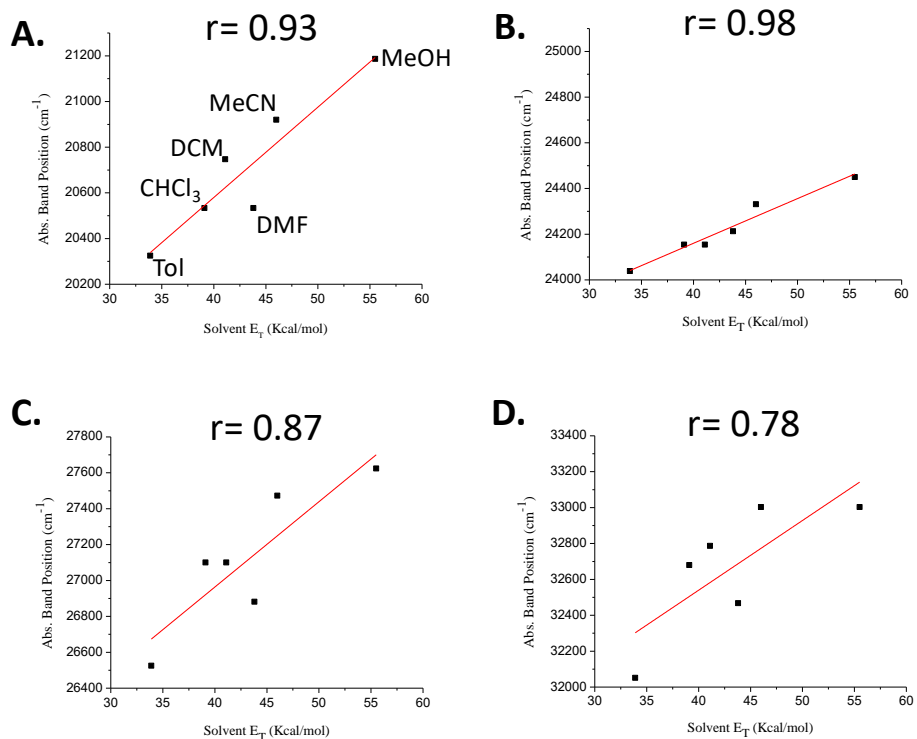
Solvent	Solvent $E_T^a$	$4g \lambda^{Abs} / \text{nm}$ ( $\epsilon, \text{M}^{-1}\text{cm}^{-1}$ )	$4h \lambda / \text{nm}$ ( $\epsilon, \text{M}^{-1}\text{cm}^{-1}$ )	$4i \lambda / \text{nm}$ ( $\epsilon, \text{M}^{-1}\text{cm}^{-1}$ )
Toluene	33.9	312(79900), 377(29000), 416(25600), 492(10700)	315(80700), 372(40600), 452(9400), 528(3600)	316(70800), 374(32200), 456(8300), 544(2700)
Chloroform	39.1	306(83600), 369(30800), 414(24400), 487(12000)	310(83600), 367(30800), 438(24400), 517(12000)	311(83600), 367(30800), 447(24400), 532(12000)
Dichloromethane	41.1	305(83600), 369(30800), 414(24400), 482(12000)	309(82100), 367(44100), 439(8700), 508(3100)	309(75900), 366(36300), 446(7700), 520(3000)
Dimethylformamide	43.8	308(73800), 372(26500), 413(21000), 487(9700)	313(73500), 369(38600), 438(7800), 520(3200)	313(68700), 370(32200), 447(7700), 532(2800)
Acetonitrile	46.0	303(76200), 364(27800), 411(20800), 478(10700)	306(66400), 363(35700), 433(7400), 502(3200)	307(57000), 362(28500), 430(6700), 514(2600)
Methanol	55.5	303(83600), 362(30800), 409(24400), 472(12000)	307(83600), 363(30800), 424(24400), 501(12000)	307(83600), 363(30800), 428(24400), 513(12000)

<sup>a</sup> Reichardt-Dimroth solvent functions (Kcal/mol).<sup>5</sup>

This solvatochromic study is an important tool to evaluate charge distribution in both ground and excited states, as well as to study Franck-Cordon phenomena.<sup>5,6</sup> Among the empirical correlations of the absorption band positions for complexes **4g-i**, we explore a measure of the ionizing power of the solvents  $E_T$  (Reichardt-Dimroth solvent functions).  $E_T$  is defined by equation 1:

$$E_T = hc\bar{v}N \quad (1)$$

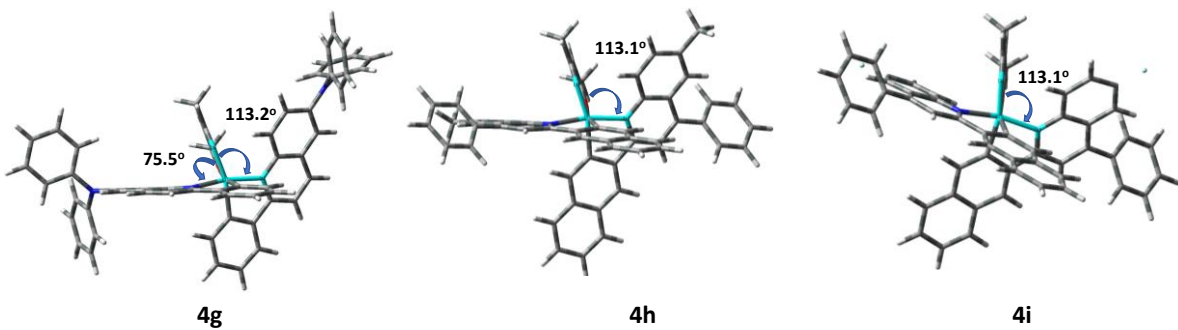
where  $h$  is the Planck's constant,  $c$  the velocity of light,  $N$  the Avogadro's number, and  $\bar{v}$  denotes the frequency of the absorption maximum.<sup>6</sup> Fig S13A-D shows the relationship between the position of the absorption bands in  $\text{cm}^{-1}$  with  $E_T$  for **4g**.



**Fig S13.** Solvent shifts of absorption band positions of **4g** with respect to the ionizing power of the solvents ( $E_T$ ): **A.** Transition band around 482 nm; **B.** Transition band around 414 nm; **C.** Transition band around 369 nm; and **D.** Transition band around 305 nm according to Table S2.

#### 2.4.2. Optimized structures

The optimized structures of **4g-i** were performed using B3LYP methods with the 6-31G(d) basis set for light atoms and LanL2DZ basis set for Ir atom.

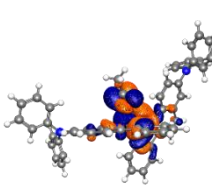
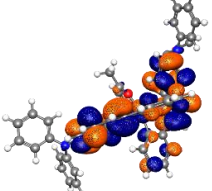
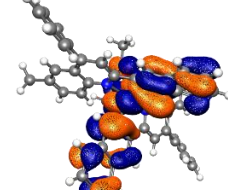
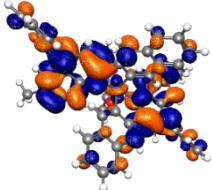
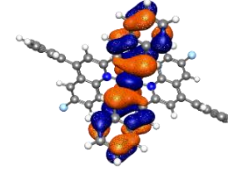
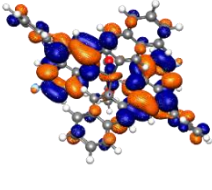
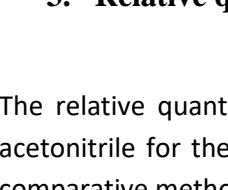
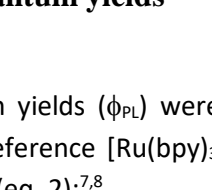


**Fig S14.** Optimized structure of the complexes **4g-i**

#### 2.4.3. Transition excited states

Transition excited states calculated using TD-DFT are shown in Table S3. The highest occupied and lowest unoccupied molecular orbital (HOMO and LUMO) energy values, and their spatial distributions for **4g-i** are also compiled in Table S3.

**Table S3.** Transition excited states calculated for the new complexes using TD-DFT

Complex	HOMO topology	LUMO topology	HOMO /eV	LUMO /eV	States	Composition	Character	E/eV[nm]	f
4g			-4.2(5)	-1.6(9)	S1	H→L [98%]	MLCT	1.79[690]	0.012
						H-1→L+1 [97%]	MLCT/LLCT/		
					S3	H→L [0.74%]	ILCT	2.04[608]	0.068
						H-4→L+1 [62%]	MLCT/ILCT		
					S7	H-3→L+1 [31%]	ILCT/MLCT		
						H-2→L [4%]	ILCT	2.80[443]	0.038
						H-1→L+3 [1%]	LLCT		
					S10	H-3→L+1 [11%]	ILCT		
						H-2→L [78%]	ILCT	2.92[425]	0.214
					S11	H-2→L+1 [65%]	ILCT		
4h			-4.2(2)	-1.8(0)		H-3→L [18%]	ILCT/MLCT	2.94[421]	0.127
					S1	H-1→L [95%]	MLCT/LLCT	1.72[721]	0.024
					S3	H→L+1 [95%]	MLCT/ILCT	1.82[681]	0.025
						H-1→L [3%]	MLCT/LLCT		
					S5	H-2→L [94%]	ILCT	2.58[480]	0.015
					S8	H-1→L+3 [47%]	MLCT/LLCT		
						H-1→L+4 [43%]	ILCT/MLCT	2.67[464]	0.015
					S9	H-4→L+1 [8%]	MLCT/ILCT		
						H-3→L+1 [70%]	MLCT	2.69[460]	0.033
						H→L+2 [12%]	MLCT/ILCT		
4i			-4.4(9)	-2.1(7)		H-4→L [9%]	MLCT/LLCT/		
						ILCT			
					S10	H-3→L [38%]	MLCT	2.70[459]	0.022
						H→L+3 [16%]	MLCT/ILCT		
						H→L+4 [20%]	MLCT/LLCT		
					S11	H-3→L+1 [10%]	MLCT		
						H→L+2 [83%]	MLCT/ILCT	2.76[450]	0.063
					S1	H-1→L [92%]	MLCT/LLCT	1.65[751]	0.018
					S3	H→L+1 [92%]	MLCT/ILCT	1.72[720]	0.026
					S5	H-1→L [6%]	MLCT/LLCT		
4j			-4.4(9)	-2.1(7)		H-2→L [94%]	ILCT	2.43[503]	0.017
						H-4→L+1 [15%]	MLCT/ILCT		
					S8	H-3→L+1 [68%]	MLCT/LLCT/		
						ILCT	2.63[471]	0.032	
						H→L+2 [13%]	MLCT/ILCT		
					S9	H-4→L [16%]	MLCT/ILCT		
						H-3→L [53%]	MLCT/ILCT	2.66[467]	0.015
					S10	H-1→L+3 [45%]	MLCT/LLCT		
						H-1→L+4 [26%]	MLCT/ILCT	2.68[463]	0.019
						H→L+2 [24%]	MLCT/ILCT		
4k			-4.4(9)	-2.1(7)		H-3→L+1 [11%]	MLCT/LLCT/		
						ILCT			
					S11	H-1→L+3 [18%]	MLCT/LLCT	2.69[421]	0.048
						H→L+2 [58%]	MLCT/ILCT		

### 3. Relative quantum yields

The relative quantum yields ( $\phi_{PL}$ ) were measured in degassed solution of dichloromethane, or acetonitrile for the reference  $[\text{Ru}(\text{bpy})_3](\text{PF}_6)_2$ , with an excitation wavelength of 420 nm using a comparative method (eq. 2):<sup>7,8</sup>

$$\phi_{PL} = \phi_{PL}^{std} \frac{IA^{std}\eta^2}{I^{std}A\eta_{std}^2} \quad (2)$$

Where  $I$  and  $I^{std}$  are the areas under the emission curves of the complexes and standard, respectively.  $A$  and  $A^{std}$  are the respective absorbances of the sample and standard at the excitation wavelengths, and  $n^2$  and  $n_{std}^2$  are the refractive indices of solvents used for the sample and standard, respectively.  $[\text{Ru}(\text{bpy})_3](\text{PF}_6)_2$  in acetonitrile ( $\phi_{PL}^{std} = 0.062$ ).

#### 4. References

- 1 Y. Liu, Y. Hu, Z. Cao, X. Zhan, W. Luo, Q. Liu and C. Guo, *Adv. Synth. Catal.*, 2018, **360**, 2691–2695.
- 2 A. G. Osborne, *Spectrochim. Acta Part A Mol. Spectrosc.*, 1983, **39**, 477–485.
- 3 W. Ahmed, S. Zhang, X. Yu, Y. Yamamoto and M. Bao, *Green Chem.*, 2018, **20**, 261–265.
- 4 S. Anvar, I. Mohammadpoor-Baltork, S. Tangestaninejad, M. Moghadam, V. Mirkhani, A. R. Khosropour and R. Kia, *RSC Adv.*, 2012, **2**, 8713–8720.
- 5 A. P. Wilde and R. J. Watts, *J. Phys. Chem.*, 1991, **95**, 622–629.
- 6 M. S. Tunuli, M. A. Rauf and others, *J. Photochem.*, 1984, **24**, 411–413.
- 7 A. T. R. Williams, S. A. Winfield and J. N. Miller, *Analyst*, 1983, **108**, 1067–1071.
- 8 S. Fery-Forgues and D. Lavabre, *J. Chem. Educ.*, 1999, **76**, 1260.